Title
MEASUREMENT OF THE MAGNETIC MOMENT AND LIFETIME OF THE 13+/2 LEVEL IN 205Pb

Authors
Maier, K.H.
Leigh, J.R.
Diamond, R.M.

Publication Date
1971-07-01

Submitted to Nuclear Physics

LBL-202
Preprint c.2

MEASUREMENT OF THE MAGNETIC MOMENT AND LIFETIME OF THE $\frac{13}{2}^+$ LEVEL IN ^{205}Pb

K. H. Maier, J. R. Leigh, and R. M. Diamond

July 1971

AEC Contract No. W-7405-eng-48

LAWRENCE RADIATION LABORATORY
UNIVERSITY of CALIFORNIA BERKELEY

MEASUREMENT OF THE MAGNETIC MOMENT AND LIFETIME OF THE $\frac{13}{2}^+$ LEVEL IN ^{205}Pb*

K. H. Maier†, J. R. Leigh, and R. M. Diamond

Lawrence Berkeley Laboratory
University of California
Berkeley, California 94720

July 1971

Abstract

The g-factor, halflife, and branching ratios of the $\frac{13}{2}^+$, 1014 keV isomer in ^{205}Pb have been measured using pulsed beam excitation through the $^{204}Hg(\alpha,3n)^{205}Pb$ reaction ($g = -0.150 \pm 0.006$, $T_{1/2} = 5.55 \pm 0.2$ ms). The implications of the result on the magnetic polarization of the core and the effective orbital g-factor of the neutron are discussed.

Nuclear Moments (static) ^{205}Pb $\frac{13}{2}^+$ 1014 keV; measured μ, $T_{1/2}$, I_γ.

*Work performed under the auspices of the U. S. Atomic Energy Commission.

†NATO fellow on leave from Hahn-Meitner-Institut, Berlin.

1. Introduction

Magnetic moments in the region around ^{208}Pb are of great interest as they show large deviations from the shell-model predictions even though this model is otherwise particularly successful for these nuclei. Many theoretical investigations to explain these deviations have been carried out[1-8]. Though all these calculations give the right trend, a quantitative description of the magnetic moments has been missing. Partly this is due to the lack of experimental data which has not allowed a test of the relative importance of the various possible causes for the deviations. So far only the g-factors for protons in $h_{9/2}$ (ref. 9) and $i_{13/2}$ (ref. 10) orbits around the ^{208}Pb core and the $p_{1/2}$ (ref. 9) and $f_{5/2}$ (ref. 11) neutron hole in this core have been measured. We have therefore determined the magnetic moments of some shell-model states in nuclei around ^{208}Pb. We were then able to reproduce all the measured moments near ^{208}Pb with an effective operator[12] that is based primarily on core-polarization effects, but also includes an anomalous orbital g-factor[10].

The present work, and a following study, aims to determine the magnetic moment of the $i_{13/2}$ neutron hole. Magnetic moments of $\frac{13}{2}^+$ levels in this region are known for the isomers in $^{193,195,197}Hg$ as $\mu = -1.05$, -1.049, and -1.032 nm respectively[9]. The Schmidt value is $\mu = -1.913$ nm. As these nuclei are rather far from ^{208}Pb, the deviation might result from various sources and is not particularly surprising. Clearly the most desirable measurement would be the moment of the $\frac{13}{2}^+$ level in ^{207}Pb which is just an $i_{13/2}$ neutron hole in ^{208}Pb. However the halflife of this level ($T_{1/2} = 0.743 \pm 0.022$ s)[13] makes this very difficult in general, and impossible for us. There are three other states whose magnetic moments can be measured and should give valuable information on the $i_{13/2}$

neutron. Nothing has been done to our knowledge on the $(\pi h_{9/2}, \nu i_{13/2}^{-1})_{10^-}$ isomer ($T_{1/2}$ = 2.5 ms) in ^{208}Bi[14]). In a separate paper[12]) we report on the g-factor measurement of the $(\nu p_{1/2}^{-1}, \nu i_{13/2}^{-1})_{7^-}$ level in ^{206}Pb, and this article is concerned with the $\frac{13}{2}^+$ level in ^{205}Pb. Neutron pick-up experiments on ^{206}Pb show that this state is a quite pure $i_{13/2}$ neutron hole, as about 90% of the ℓ=6 strength is exhausted by this level[15,16]). To test further the purity of the wave function of this state we also measured its lifetime and the branching ratios, which were not known accurately. Of special interest is the partial halflife of the $\frac{13}{2}^+$ (M4) $\frac{5}{2}^-$ decay, since this corresponds to the decay mode of the $\frac{13}{2}^+$ level in ^{207}Pb. The decay scheme of the isomer is shown in fig. 1. Its qualitative features, energies, spins, and multipolarities had been established already, and are taken from ref. 9, while the halflife and intensities given are the results of this work.

2. Experimental

The experiments were performed at the Berkeley Hilac. The isomer was produced through the reaction $^{204}Hg(\alpha,3n)^{205}Pb$ with 41 MeV α-particles on a thick liquid ^{204}Hg target (enriched to 80%) which is described in ref. 12. The γ-rays were detected with a 35 cm^3 coaxial Ge(Li) detector. As will become clear from the discussion of the g-factor measurement, electronics that recover rapidly from heavy overloading during the beam pulses were necessary to make the experiments possible. This was accomplished in two steps: (i) a circuit was installed in the preamplifier that discharged the feedback capacitor before the preamplifier saturated: (ii) a gate at the input of the main amplifier was disabled during the beam pulse to prevent overloading this unit. These changes made it possible to start measuring some ten microseconds after the beam pulse with a resolution of 4 keV for 1 MeV γ-rays. The main amplifier is followed by a linear gate that is controlled by a pile-up rejector. The actual measuring interval is determined by applying a gate signal to a coincidence circuit incorporated in the pile-up rejector. For the measurements of the energy spectrum the output of the linear gate was fed through a three-fold derandomizing analog storage unit to a 4096 channel ADC. For the time measurements only the strong 988 keV line was used, and it was singled out by means of a biased amplifier and single-channel analyzer following the linear gate. The output of this analyzer then sampled a linear ramp initiated by the beam pulse. These linear time signals were also fed through a derandomizer into a 512-channel ADC. Thus it was possible to count many events after each beam pulse, as compared to only one with standard time-to-pulse-height conversion techniques. The pile-up rejector was the cause of the 6 μs deadtime of the system, since the derandomizer makes the ADC deadtime unimportant. The spectra were accumulated in a PDP-7 on-line computer.

3. Results

3.1. HALFLIFE MEASUREMENT

The normal Hilac beam structure, a 4-5 ms pulse repeated 36 times per second was used. The time-measuring system was calibrated with a quartz oscillator before and after the experiment. The evaluation was done by integrating the counts over 1 ms intervals determined by the oscillator. There was practically no background under the 988 keV peak observed by the Ge(Li) detector. The results of two runs with the beam level differing by a factor of 4 are shown in fig. 2, together with best fits to a pure exponential. The two results differ by 3%, which cannot be explained by statistics, and for which we have no explanation. We therefore give the halflife as: $T_{1/2} = 5.55 \pm 0.2$ ms.

3.2. BRANCHING RATIOS

Simultaneously with the halflife measurement a gamma-ray spectrum was recorded in the interval from 1 to 5 ms after the beam pulse. It is shown in fig. 3. Except for the 26 keV M2 transition, all the lines from the decay of the isomer can be seen. The efficiency curve for this experimental arrangement with the approximately 0.5 g/cm^2 mercury target is not known very accurately. Fortunately, we have to compare only the high-energy lines at 703, 988, and 1014 keV, which should be only slightly influenced by absorption in the target, and the two close-lying lines at 284 and 310 keV (see fig. 1). Since the 310 keV E3 transition is weak, the branching ratio of the $\frac{9}{2}^-$ level can be determined from the 703 and 988 keV line. The relative intensities of the M4 and E3 branches from the isomer can then be taken from the intensity ratios of the 1014 to 988 keV and 310 to 284 keV lines, respectively. The results for the total intensities of the transitions including internal conversion, and normalized to 85 for the 988 keV E2, with an implied intensity of 100 ± 5 for the 26 keV M2 transition, are: 310 keV: 1 ± 0.5; 284 keV: 15 ± 5; 703 keV: 15 ± 5; and 1014 keV: 0.59 ± 0.09. The partial halflife for the M4 transition is then (0.94 ± 0.15) s and that of the E3 transition is (550 ± 300) ms.

3.3. MEASUREMENT OF THE g-FACTOR

The g-factor was measured by the method of differential perturbed angular distributions following reactions (DPAD). In this, the isomer is produced and aligned by means of a nuclear reaction induced by a pulsed beam. A magnetic field H is applied to the target perpendicular to the beam axis, and causes a Larmor precession of the nuclei ($\omega_L = -g.H. \frac{\mu_N}{\hbar}$). The angular distribution of the de-exciting γ-rays rotates likewise. Therefore a detector positioned in the plane perpendicular to the magnetic field direction shows a sinusoidal modulation of the count rate superimposed on the exponential decay:

$$I(t,\theta) = \exp(-\lambda t)\left(1+\exp(-\rho t)A_2P_2(\cos(\theta-\omega_L t))\right) \quad . \qquad (1)$$

Here t is the time elapsed from the centroid of the beam pulse, θ is the angle between the detector and the beam direction, λ is the decay constant and A_2 is the angular distribution coefficient of the observed transition. Higher terms than P_2 in the angular distribution are neglected since they are small. For the lifetime encountered here, relaxation phenomena are important, and with the liquid target result in an exponential decay of the anisotropy characterized by a decay time $T_R = 1/\rho$. From previous experiments[12]), T_R could be estimated to be about 0.5 ms. The following conditions have to be fulfilled for the present measurement: Δt (width of beam pulse) << $T = \frac{\pi}{\omega_L}$ (period of rotation of the angular distribution) << T_R, and T_{rep} (repetition time of the beam) >> $T_{1/2}$. For an estimated g-factor of -0.1 and a field of 50 G, the time for one revolution of the angular distribution would be $T = 130$ μs, so beam pulses of width $\Delta t = 20$ μs were used. The beam repetition time was $T_{rep} = \frac{1}{36}$ s. Thus the measuring time was about 2% of the real time and the beam-on time was only 0.07%. In order to make the experiment feasible in a reasonable period of time, the beam current during the pulse had to be 2 to 3 orders of magnitude larger than we normally used for in-beam γ-ray studies.

With such a beam current, the fast-recovering electronics described above were absolutely necessary. The beam itself was pulsed by applying a square-wave voltage to a pair of deflection plates located between the injector and the prestripper tank of the Hilac. The magnetic field at the target was provided by a small electromagnet and measured by integrating the current induced in a coil that was flipped in the field. This device was calibrated before and after the run in a precisely known field.

The time distribution of the 988 keV line as accumulated in 8 hours of running is shown in fig. 4. The measuring interval started about 50 μs after the beam pulse and was 1.1 ms wide. The 50 μs delay was necessary mainly because of the strong excitation of the 7^- isomer in ^{206}Pb ($T_{1/2}$ = 120 μs) through the ^{204}Hg(α,2n)-reaction in the thick target. The initial rise seen in the time distribution is due to the deadtime introduced in the pile-up rejector by this isomer. The background under the 988 keV line was less than 5%. Though the oscillations due to the Larmor precession are clearly visible in fig. 4 an evaluation according to eq. (1) is difficult due to the deadtime distortion of the spectrum. Therefore the standard procedure of positioning the detector at 45° and measuring with the field both up and down while everything else is kept constant was used. One then can evaluate the ratio:

$$\frac{I(H\uparrow) - I(H\downarrow)}{I(H\uparrow) + I(H\downarrow)} = \frac{3A_2 \exp(-\rho t) \sin(2\omega_L t)}{4 + A_2 \exp(-\rho t)} \quad . \tag{2}$$

In this expression the common deadtime distortion cancels, together with the exponential describing the decay, and essentially a damped sine wave is left as the denominator varies smoothly and by less than 10%. Figure 6 gives the experimental left-hand side of eq. (2) together with a best fit according to the right side. For the actual fitting procedure an arbitrary phase of the sine had to be introduced as the time zero was only determined with sufficient accuracy to give the sign of g.

Actually at $\theta = 45°$ only the sign of the product of A_2 and g is determined. However, we checked in a separate experiment that the sign of A_2 is positive, as expected for a stretched E2-transition. The results are: $g = -0.150 \pm 0.004$, $A_2 = +0.3$, $T_R = 0.4 \pm 0.2$ ms. The errors of g and T_R are estimated from fitting different portions of the time distribution. The errors of the field measurement and the calibration of the time scale, accomplished with a quartz crystal oscillator, are unimportant. The apparent g-factor has to be corrected for a diamagnetic and Knight shift of the field at the nucleus. The Knight shift for lead in liquid mercury can only be estimated from the known shifts for mercury in mercury (2.4%)[17] and lead in lead (1.5%)[17]. It turns out that it just cancels the diamagnetic shift (-1.7%)[18]. However, an additional error of 1% has been allowed for these corrections. Thus the final result is:

$$g(13/2^{+}\ {}^{205}\mathrm{Pb}) = (-0.150 \pm 0.006) \quad \text{(corrected)} \quad ,$$

which corresponds to a magnetic moment, $\mu = (-0.975 \pm 0.040)$ nm.

4. Discussion

Before considering the measured magnetic moment, we have to discuss the wavefunction of the $\frac{13}{2}^+$ level. Two studies of the neutron pick-up process on ^{206}Pb with the (p,d) and (d,t) reaction consistently give the spectroscopic factor for the $^{206}\mathrm{Pb} \rightarrow \frac{13}{2}^+\ ^{205}\mathrm{Pb}$ transition as 90% of the corresponding transition from ^{208}Pb to ^{207}Pb[15,16]. The B(M4) value of the $\frac{13}{2}^+$ (M4) $\frac{5}{2}^-$ transition amounts to (115 ± 20)% of the analogous transition in ^{207}Pb, again suggesting that the $\frac{13}{2}^+$ state in ^{205}Pb is rather pure and similar to the one in ^{207}Pb. The hindrance of 2 to 3 orders of magnitude for the M2 and E3 branches from the isomer is reasonable, since these transitions proceed to levels which should have very small single-particle components and indeed are not seen at all in the pick-up experiments.

For the discussion of the magnetic moment, therefore, we will assume that the wavefunction of the $\frac{13}{2}^+$ level in ^{205}Pb is about 90% an $i_{13/2}$ neutron hole in a ^{206}Pb 0^+ core. For the remaining 10%, the configurations $(i_{13/2}, 2^+)_{13/2^+}$ and $(f_{7/2}, 3^-)_{13/2^+}$, the main admixture in ^{207}Pb, are the most likely candidates. The magnetic moments of these admixtures should certainly have the same sign and probably even roughly the same magnitude as that of the main component. Therefore, the measured magnetic moment should be within about 10% of that of the pure $i_{13/2}$ neutron hole. In a recent article[12] we derived an effective magnetic-moment operator for single-particle levels around a ^{208}Pb core. This derivation used the magnetic moment of the $i_{13/2}$ neutron calculated from the measured moments of the ^{207}Pb ground-state $(p^{-1}_{1/2})$ and the $(p^{-1}_{1/2}, i^{-1}_{13/2})_{7-}$ isomer in ^{206}Pb, assuming additivity. The four numbers to be compared are: (a) $\mu(i^{-1}_{13/2}) = -0.75$ nm from the ^{206}Pb level; (b) -0.975 nm from ^{205}Pb; (c) the Schmidt value of -1.91 nm; and (d) the prediction of the effective operator, -0.62 nm.

Both measurements agree to 0.2 nm compared to the 1 nm deviation from the Schmidt value. This means that the essential points of the discussion in ref. 12 need not be changed at all. On the contrary, the agreement helps remove the doubts one might have had on the validity of the evaluation of the moment from that of a two-particle level on the basis of additivity of moments. The deviation of 0.2 nm might be caused by impurities in the wavefunctions, particularly of the 7^- state in ^{206}Pb.

The deviation of the present measurement from the prediction of the effective operator is -0.35 nm, which is larger than the deviations found for the other four single-particle moments (< 0.1 nm) used for evaluating the parameters of the effective operator. But the predicted value was calculated assuming an orbital g-factor for the neutron of zero. Using a value of -0.05 gives agreement for the present case without harming appreciably the fits to the other moments. If the somewhat smaller g-factor derived from the measurement on the 7^- state in ^{206}Pb is also taken into account (leading to a smaller δg_ℓ), as well as the uncertainties involved in their interpretation, the only quite safe statement is $-0.1 < \delta g_{\ell n} < 0$.

This value does seem, however, to be in agreement with the statement of Yamazaki <u>et al</u>.[10]) that if the anomalous orbital g-factor is assumed to be due to mesonic currents, it is an isovector and so $\delta g_{\ell n} = - \delta g_{\ell p}$. But because the number of neutrons and protons are different in the region around ^{208}Pb, the value for neutrons will be reduced by the Pauli principle to roughly Z/N the proton value. So $\delta g_{\ell n} = -0.06$ might be expected[19,†]).

†The g-factor of the $(\nu^{-2}_{13/2})_{12^+}$ isomer in ^{206}Pb has just been determined by a Copenhagen-Stockholm collaboration[20]) as $g = -0.152 \pm 0.004$. This is in agreement with the present result, as is their conclusion that the orbital g-factor of the neutron is about -0.03.

Acknowledgments

We want to thank Drs. F. Stephens, K. Nakai, and J. Quebert for their help with part of the measurements, and Mr. P. Watson and the magnet test group for their assistance in the field measurement. We are especially obliged to Mr. Jack Walton and Mr. Don Landis for developing the fast-recovering electronics that made this experiment possible. One of us (K.H.M.) wants to thank the Deutscher Akademischen Austauschdienst for supplying the fellowship for his stay.

References

1) A. Arima and H. Horie, Progr. Theoret. Phys. 11 (1954) 509

2) R. J. Blin-Stoyle and M. A. Perks, Proc. Phys. Soc. (London) A67 (1954) 885

3) E. Bodenstedt and J. D. Rogers in, Perturbed Angular Correlations, eds. E. Karlsson, E. Matthias, and K. Siegbahn, (North-Holland Publishing Co., Amsterdam, 1964) p. 93

4) B. R. Mottelson, Nordita publications, No. 288, p. 54

5) J. Blomqvist, N. Freed, and H. O. Zetterström, Phys. Letters 18 (1965) 47

6) A. Bohr and B. R. Mottelson, Nuclear Structure, (Benjamin Inc., 1969, New York, Amsterdam), Vol. I, p. 336

7) K. Harada and S. Pittel, Nucl. Phys. A159 (1970) 209

8) Further references given in 1-7

9) C. M. Lederer, J. M. Hollander, and I. Perlman, Table of Isotopes (Wiley & Sons, 1967, New York)

10) T. Yamazaki, T. Nomura, S. Nagamiya, and T. Katou, Phys. Rev. Letters 25 (1970) 547

11) H. J. Körner, K. Auerbach, J. Braunsfurth, and E. Gerdau, Nucl. Phys. 86 (1966) 395

12) K. H. Maier, K. Nakai, F. S. Stephens, and R. M. Diamond, to be published

13) H. P. Yule, Nucl. Phys. A94 (1966) 442

14) W. Gabsdil, Nucl. Phys. A120 (1968) 555

15) R. Tickle and J. Bardwick, Phys. Rev. 178 (1969) 2006

16) K. Yagi, T. Ishimatsu, Y. Ishizaki, and Y. Saji, Nucl. Phys. A146 (1970) 215

17) L. E. Drain, Met. Rev. 12 (1967) 195

18) F. D. Feiock and W. R. Johnson, Phys. Rev. Letters 21 (1968) 785

19) T. Yamazaki and S. Nagamiya, private communication (1971)

20) K. Nakai, private communication (1971)

Figure Captions

Fig. 1. Decay scheme of the $13/2^+$ isomer in ^{205}Pb. Spins, multipolarities, and energies are from ref. 9.

Fig. 2. Halflife measurement of the $13/2^+$ isomer in ^{205}Pb. Both curves show the intensity of the 988 keV line. The lower set of points was taken at a beam level reduced by a factor of 4; the vertical scale has to be divided by 10 for these points. The two best fits that are shown give the halflife as 5.62 ms (upper curve) and 5.47 ms (lower curve). Statistical errors are within the size of the points.

Fig. 3. Energy spectrum of γ-rays from the decay of the $13/2^+$ isomer in ^{205}Pb.

Fig. 4. g-factor measurement of the $13/2^+$ level in ^{205}Pb. Time distribution of the 988 keV line. The interval shown starts about 50 μs after the beam pulse.

Fig. 5. The ratio $(I(H\uparrow)-I(H\downarrow))/(I(H\uparrow)+I(H\downarrow))$ together with the least-square fit.

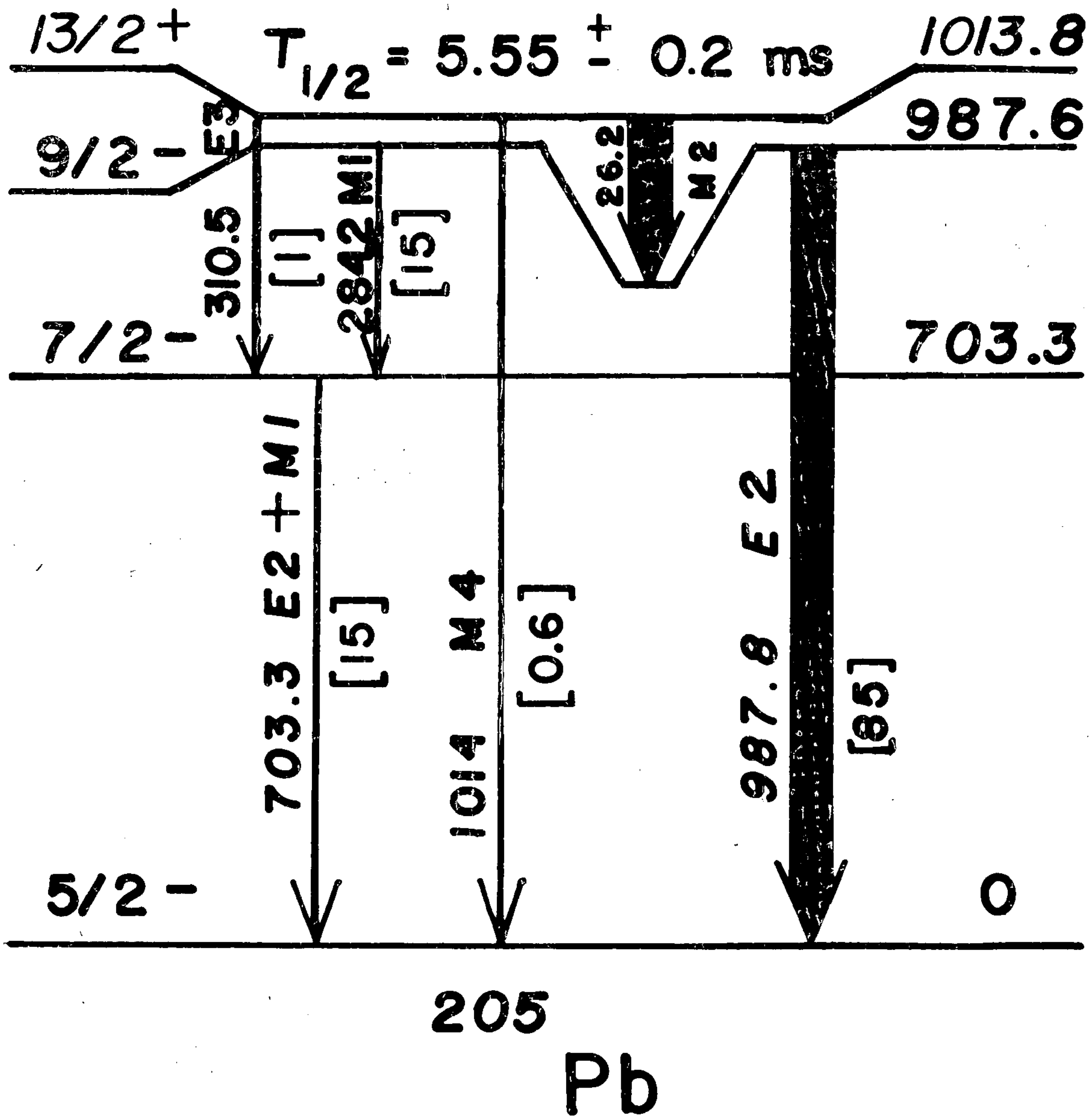

XBL 712-218

Fig. 1

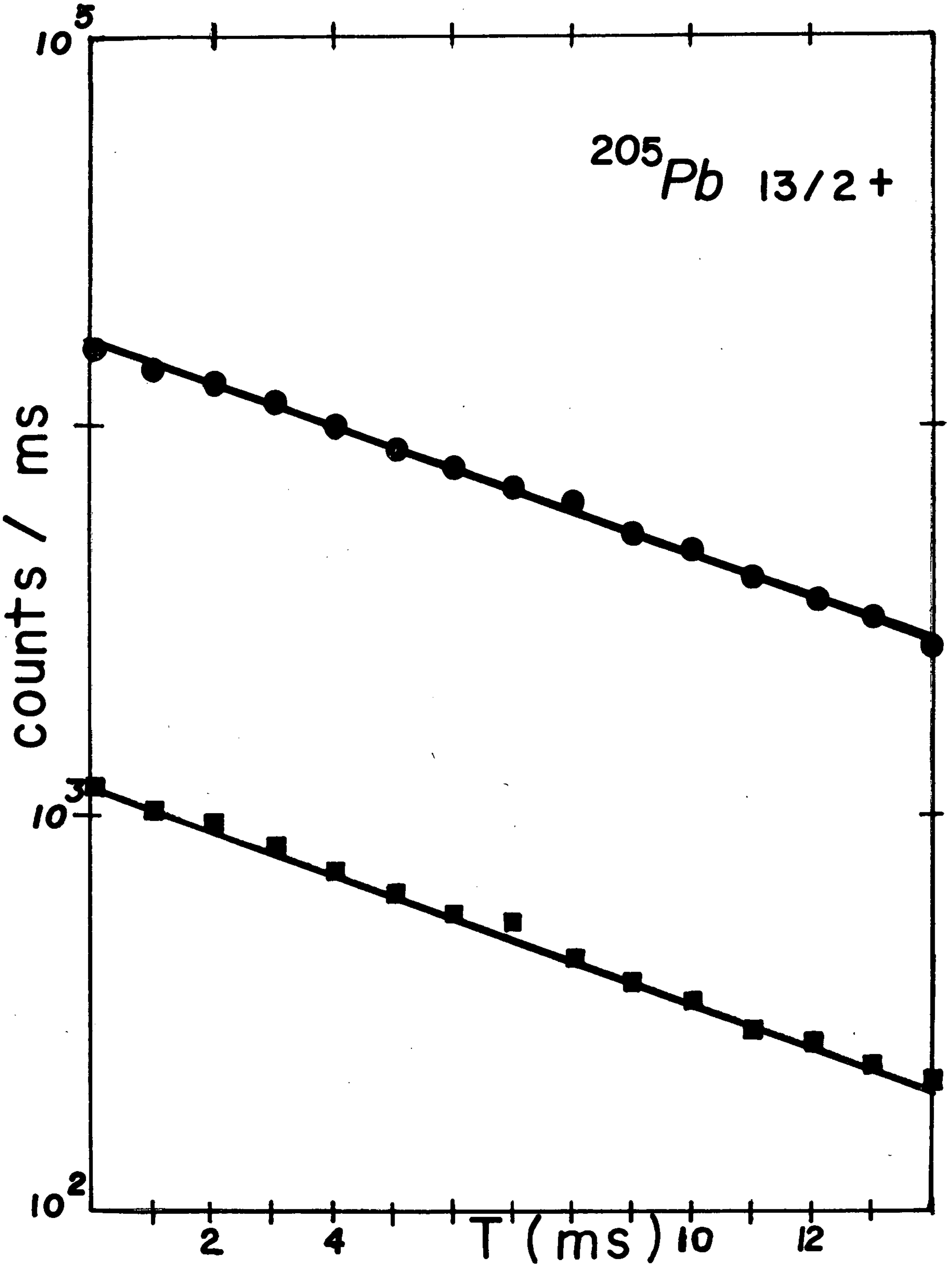

XBL 712-219

Fig. 2

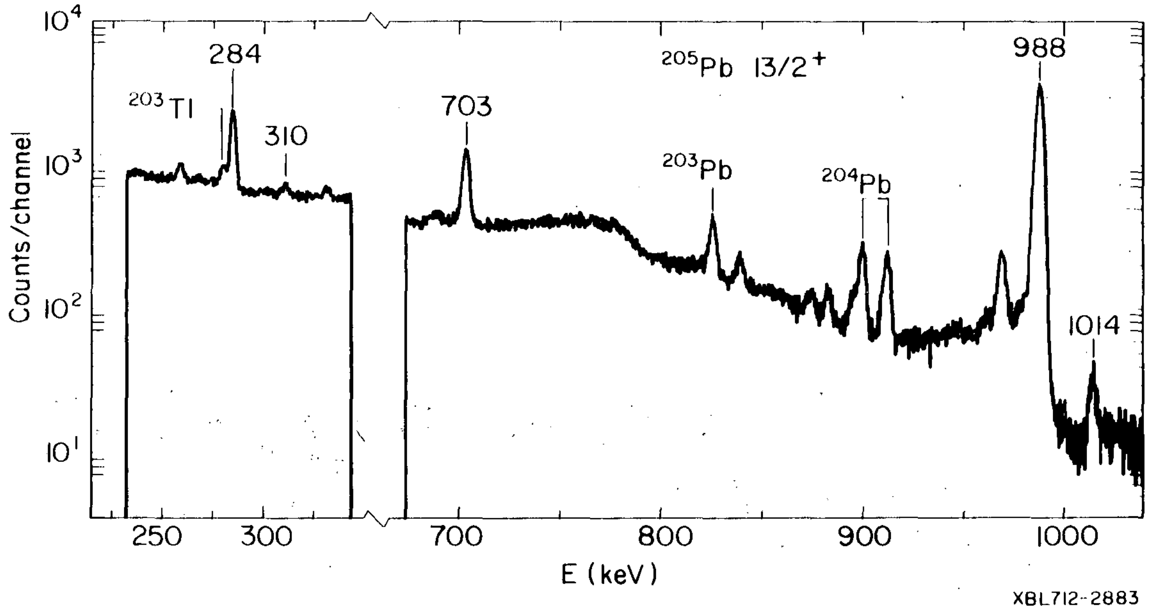

10^4
10^3
10^2
10^1
Counts/channel
284
^{203}Tl
310
703
^{205}Pb 13/2$^+$
^{203}Pb
^{204}Pb
988
1014
250
300
700
800
900
1000
E (keV)
XBL712-2883

Fig. 3

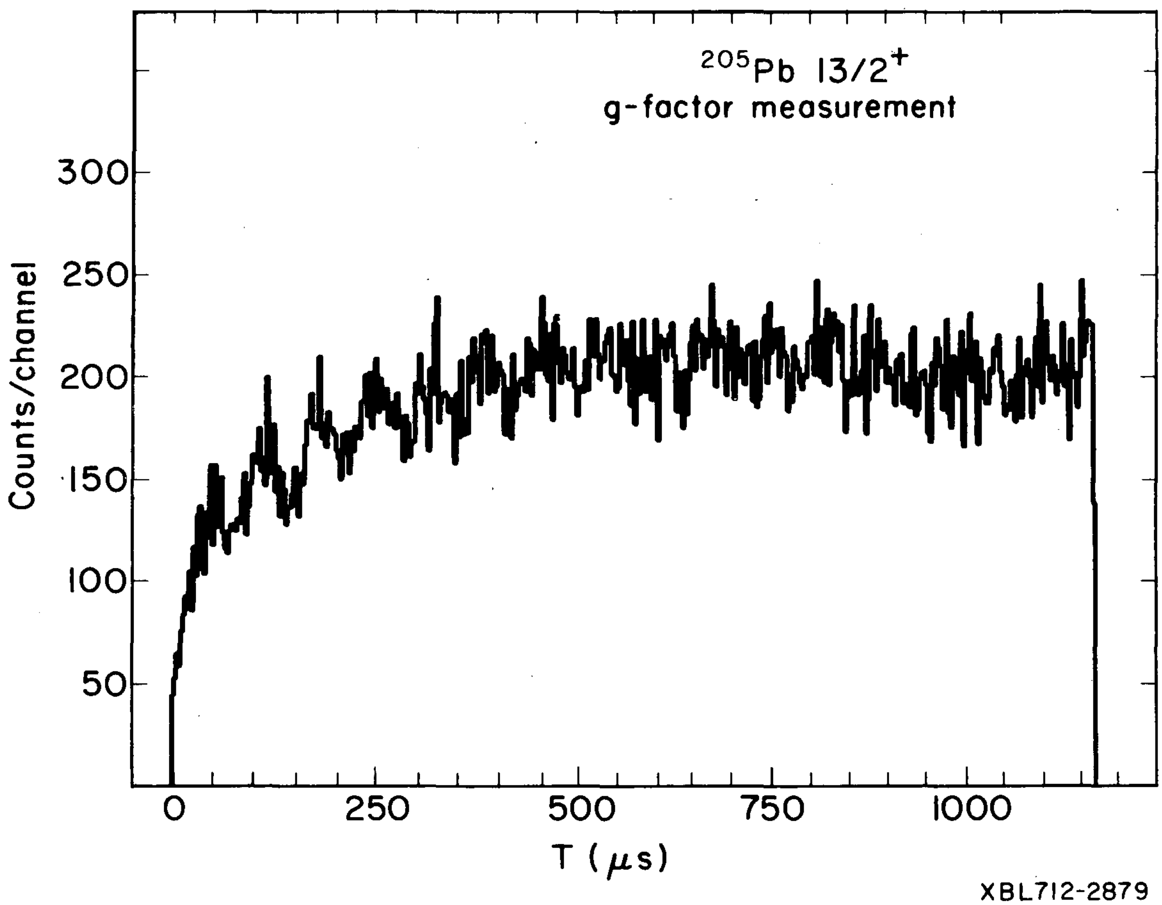
205Pb 13/2+
g-factor measurement
Counts/channel
300
250
200
150
100
50
0
250
500
750
1000
T (μs)
XBL712-2879

Fig. 4

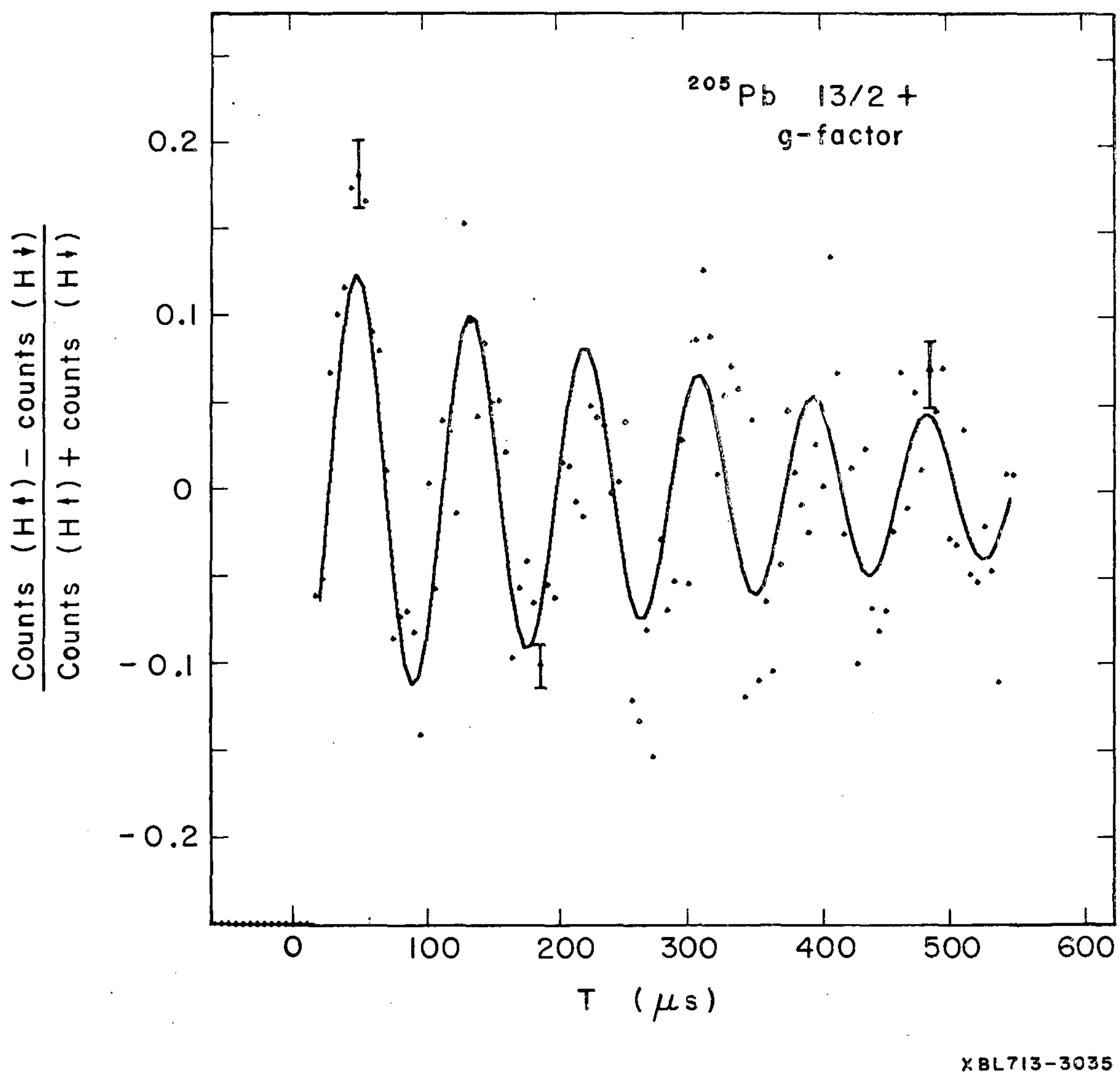

205Pb 13/2 +
g-factor
0.2
0.1
0
-0.1
-0.2
0
100
200
300
400
500
600
T (μs)
Counts (H↑) − counts (H↓)
Counts (H↑) + counts (H↓)
XBL713-3035

Fig. 5

TECHNICAL INFORMATION DIVISION
LAWRENCE BERKELEY LABORATORY
UNIVERSITY OF CALIFORNIA
BERKELEY, CALIFORNIA 94720